Novel idea of neutron polychromator and application for reflectometry and spectroscopy

Norifumi L. Yamada*

Institute of Materials Structure Science, High Energy Accelerator Research Organization (KEK), Ibaraki 305-0801, Japan

Abstract. Historically, two methods have been used to determine the wavelength of neutrons: (i) a time-of-flight method that separates the velocity of pulsed neutrons by the flight time; and (ii) a method utilizing Bragg reflection by a monochromator, such as a single crystal or multilayer mirror. The former cannot be applied to electromagnetic waves because the light velocity is constant and independent of the wavelength, whereas "polychromators" such as prisms and gratings, which separate wavelengths via chromatic dispersion, are typically used in the infrared to soft X-ray range. Although polychromators require collimated beams to separate wavelengths with sufficient resolution, this aspect does not affect laser and synchrotron light because they are naturally collimated. Herein, we propose a novel idea of a neutron polychromator utilizing an elliptical multilayered mirror that can be applied to a wide beam with a large beam divergence. In addition, examples of reflectometer and spectrometer applications are presented.

1 Introduction

Historically, two methods have been used to determine the wavelength of neutrons: the time-of-flight (TOF) method, which separates the velocity of pulsed neutrons by the flight time, and a method utilizing Bragg reflection by a monochromator, such as a single crystal or multilayer mirror. The former is extremely useful for obtaining the spectrum of a white beam, i.e., the wavelength dependence of the intensity; however, it cannot be applied to electromagnetic waves because the light velocity is constant and independent of the wavelength. Hence, "polychromators" such as prisms, gratings, and bent crystals are typically used in the infrared to X-ray range.

A prism is the simplest polychromator, in which the relationship between the angles of incidence θ_{in} and extraction θ_{out} can be described as a function of wavelength λ, as follows:

$$\cos\theta_{in} = n\cos\theta_{out},$$

$$n = \sqrt{1-\frac{\lambda^2\rho}{\pi}} \sim 1-\frac{\lambda^2\rho}{2\pi} \quad (\lambda^2\rho \ll 1),$$

where n and ρ are the refractive index and scattering length density of the prism, respectively. Based on this relation, the λ dependence of the intensity can be acquired by measuring the intensity of a beam spreading out from the prism with various θ_{out} when a white beam with incident angle θ_{in} is introduced on the prism surface. However, if the beam passes through the prism in this geometry, the abovementioned method cannot be applied to X-rays because the beam is attenuated in the transmission geometry.

A grating with reflection geometry is a typical polychromator used for soft X-rays, in which the beam is not required to pass through a material. Here, the relationship between θ_{in} and θ_{out} satisfying Bragg's law of the line and the space patterns of the grating can be expressed as

$$d(\cos\theta_{in} - \cos\theta_{out}) = m\lambda,$$

where d is the repeat distance of the grating and m is the order of the Bragg peaks. Based on this relation, the λ dependence of the intensity can be acquired by counting the intensity based on θ_{out}, as in the case of a prism. As the value of d ranges from submicrons to several microns, this method cannot be applied to hard X-rays because λ is extremely small to separate, and the critical angle for the total reflection is extremely small as well.

Hard X-rays can be applied to a bent crystal [1] based on Bragg's law.

$$2d\sin\theta_{in} = m\lambda \ (\theta_{in} = \theta_{out}).$$

In this method, the distribution of θ_{in} depends on the position on the crystal because the crystal has curvature. If the beam is focused at the sample position, then it spreads to the detector position, depending on the position where the beam is reflected at the crystal. Consequently, the X-ray wavelength depends on the detection position, as in the case of the aforementioned methods.

The principle of these polychromators is applicable to neutrons; however, these polychromators are barely used for neutrons. This is attributable to the fact that they require "collimated beams" to suppress the distribution of θ_{in}, which worsens the λ resolution. In the cases of laser and synchrotron light, this feature does not impose a significant effect because the beam is naturally collimated. However, this results in a considerable

* Corresponding author: norifumi.yamada@kek.jp

decrease in the intensity of neutrons because they naturally diverge from the source. In other words, polychromators can be applied to instruments that utilize a collimated beam, such as a reflectometer. To the best of our knowledge, the only full-scale neutron instrument that uses a polychromator is the RAINBOWS reflectometer, which is equipped with a prism to capture the spectrum of narrow and collimated white neutrons reflected at a sample surface [2]. However, this restriction is not suitable for other instruments and is the biggest barrier hindering the use of polychromators in neutron instruments.

To overcome the problem, the author proposes the novel concept of a neutron polychromator comprising an elliptical multilayered mirror that can be used for neutrons with a large beam divergence. To fully exploit the polychromator with a higher order reflection and high wavelength resolution, a novel "crystallic multilayered mirror" is proposed. Furthermore, some ideas for neutron instruments utilizing a polychromator are presented: (i) a reflectometer at a continuous source, and (ii) a quasi-elastic neutron spectrometer at a pulsed source.

2 Concept of Novel Polychromator

2.1 Optics

Figure 1 shows a schematic illustration of the novel polychromator proposed herein, which comprises an elliptical focusing mirror coated with a multilayer having a periodic thickness and a position-sensitive detector (PSD). A virtual source is placed at the focal point of the mirror, and the PSD is placed at the other focal point. The image of the source is transferred to the PSD at the same magnification when the mirror is placed at the center of the focal points. In this polychromator, the incident angle on the mirror depends on the position of the virtual source. This indicates that neutrons propagating from a point closer to the mirror on the virtual source are reflected with a smaller incident angle at the mirror and are transferred to a point closer to the mirror on the PSD. Because the wavelength satisfying the Bragg reflection depends on the incident angle, the spectrum of the white beam can be observed on the detector as a function of the detection position. This is the essential idea of the novel polychromator with an elliptical mirror, which is based on the simple Bragg's law and allows a diverged beam from the virtual source to be used.

Prior to this study, the combination of elliptic mirror and multilayer as a polychromator for neutron reflectometry was proposed by Ott *et al.* [3]. In the study, they performed a Monte Carlo simulation with the optics that the beam size at the source was limited but a large focusing mirror was used. Because the incident angle to the mirror gradually increases with the distance from the center of the ellipse, the wavelength satisfying the Bragg condition also increases in the same manner. On the other hand, the wavelength dependence on the position is assumed to be corrected by controlling the layer thickness to compensate the wavelength satisfying the Bragg condition for the polychromator in this study. This correction allows us to use the monochromatic beam with the large beam divergence, while the beam divergence of a limited wavelength is very narrow before the correction. As a result, the polychromatic beam of the corrected polychromator with a wide virtual source can increase the beam flux compared to that of the previous work.

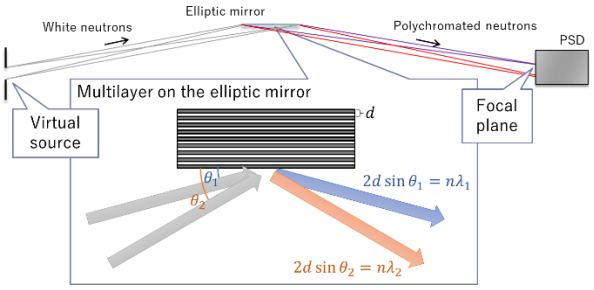

Fig. 1. Schematic illustration of the novel polychromator comprising an elliptic focusing mirror and PSD.

2.2 Crystallic multilayer

The wavelength resolution of the polychromator shown above is limited by two factors: the spatial resolution of the image on the detector, which is primarily governed by the detector resolution and the slope error of the focusing mirror; and the width of the Bragg reflection of the multilayer on the focusing mirror. The former can be reduced to less than 1% by applying the most recent technology, such as focusing mirrors via ultraprecise machining [4-6] and employing scintillation detectors [7]. Meanwhile, the width of the Bragg reflection of multiple layers of typical mirrors such as Ni/Ti remains at approximately several percent because no attempt has been made to obtain better resolutions, presumably because of the low demand for high-resolution monochromators composed of multilayers. However, polychromators require higher resolutions than monochromators as shown later. Hence, a novel method for improving the wavelength resolution of multilayers is proposed herein.

A typical multilayer mirror for non-polarized neutrons comprises Ni ($\rho = 9.4 \times 10^{-4}$ nm^{-2}) and Ti ($\rho = -1.9 \times 10^{-4}$ nm^{-2}) layers, which allows high reflectivity to be achieved using only a few of those layers owing to the high contrast in the scattering length density, i.e., the refractive indexes between the layers. On the other hand, the effective number of layers contributing to Bragg reflection is limited because of the high reflectivity, which implies that neutrons satisfying the Bragg condition cannot reach the deep layers. As the peak width of the Bragg peak decreases with an increase in the effective number of layers, the multilayer with a large stacking number composed of materials providing less reflectivity in one layer unit is expected to exhibit sharp Bragg peaks because of improved crystallinity. Hereinafter, multilayers with high crystallinity are referred to as "crystallic multilayer."

To demonstrate the concept of the crystallic multilayer, we estimated the reflectivity using the Motofit software [8] based on Parratt's recursive

method [9]. To decrease the reflectivity in one unit layer, Ge ($\rho = 3.6 \times 10^{-4}$ nm^{-2}) and Ti with asymmetric layer thickness were combined to reduce the contrast in the refractive index and enhance the tunneling of neutrons by thinning Ti layers while maintaining the periodic distance at 20 nm. The solid line in Fig. 2 shows the result of the reflectivity estimation as a function of momentum transfer along the depth direction, in which the layer thicknesses of Ge and Ti were 18.8 and 1.2 nm, respectively, and the number of unit bilayer was 2000 layers. The resolution evaluated from the full width at half maximum of the Bragg peak was 0.7% at the first peak and decreased significantly with the increasing order of the peaks, reaching 0.004% while maintaining a reflectivity of approximately 100% at the 10th peak, as shown by the circles on the right axis.

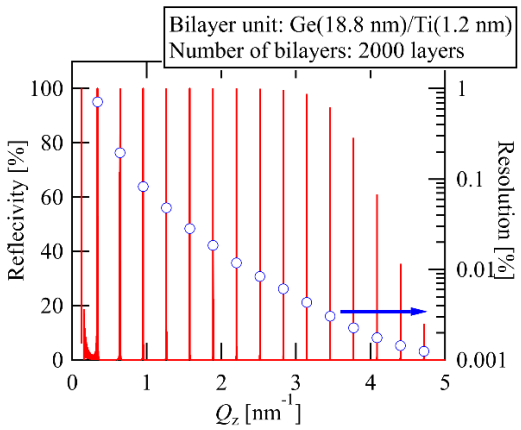

Fig. 2. Ideal reflectivity of crystallic multilayer composed of Ge/Ti bilayer (solid line, left axis) and resolution evaluated from full width at half maximum of Bragg peak (circles, right axis).

The results above are only an estimation, and the effect of microscopic roughness at the interfaces, the macroscopic inhomogeneity over the mirror, and the difference in the incident angle with respect to the position in the ellipse of the polychromator should be considered. Therefore, further research is required to realize such high resolutions by creating a multilayer with low roughness to suppress reflectivity loss and off-specular scattering, and by implementing a well-controlled thickness to compensate for the distribution of the incident angle. These ideas will be considered in future studies as the purpose of the current study is to propose a conceptual design for a novel polychromator.

3 Possible Neutron Scattering Instruments Using the Polychromator

3.1 Neutron Reflectometer

The concept of a polychromator was discussed in the previous section. Next, the possible designs for neutron scattering instruments are presented.

The design of a neutron reflectometer with a polychromator as a continuous source, which is one of the simplest designs, is considered. The principle of the instrument is extremely simple: neutrons collimated in the direction of reflection are introduced into a sample surface or interface with a small incident angle, and neutrons reflected at the sample with a reflection angle that is the same as the incident angle are counted using a detector. Because the beam is collimated and its path is finely defined, polychromators are applicable to reflectometers at a relatively low cost. Prism reflectometry has already been realized using a RAINBOWS reflectometer with a continuous source at the ILL, in which neutrons are polychromated in the direction of the reflection angle using a prism [2]. This enables us to perform rapid measurements using intense white neutrons without intensity loss using the TOF method. However, the position sensitivity in the direction of the reflection angle is diminished, which prevents us from correcting the incident angle distribution caused by beam divergence or wavy surfaces and the reflection angle caused by off-specular scattering. Also, the concept of the REFocus reflectometer using a polychromator consisting of an elliptic mirror and multilayer monochromator is proposed. This reflectometer can accept a polychromatic beam with a wide incident angle to measure the reflectivity in a wide momentum transfer range at the same time. On the other hand, by using the wide incident angle, the specular signal is disturbed by the surface waviness and the off-specular signal is buried in the specular signal.

Figure 3 illustrates the design of the neutron reflectometer with the novel polychromator for solving the problems of the reflectometers above. A sample is placed immediately in front of the elliptical mirror and reflected neutrons are polychromated in the width direction, which is insensitive to the reflection angle, not in the direction of the reflection angle. This configuration enables us to independently evaluate the wavelength of neutrons by their position on the x-axis on the detector coordinate and the sum of the incident and reflection angles of neutrons by their position on the y-axis. In other words, the degree of freedom in the x-axis position is utilized to determine the wavelength. This causes intensity loss as compared with when the RAINBOWS geometry is used, in which a homogeneous white beam propagates in the x-axis direction. However, the new geometry of the polychromator offers a significant advantage, i.e., it allows more information concerning the incident and reflection angles to be obtained. This is beneficial to the application of reflectometry to various samples and conditions for correcting the incident and reflection angles, as mentioned previously. For example, an incident beam with a large beam divergence can partially compensate for intensity loss.

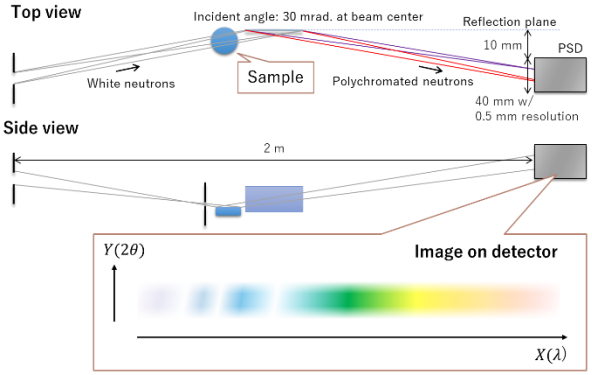

Fig. 3. Design of neutron reflectometer utilizing the novel polychromator proposed herein.

Next, the performance of the reflectometer with a polychromator is estimated. The wavelength separated by the polychromator is expressed as

$$\lambda_m = \frac{2d \sin\theta_{in}}{m} \sim \frac{2dx}{mL},$$

where x is the distance from the detection position to the reflection plane at the polychromator center, L is the flight distance from the polychromator to the detector, and the subscript m of λ represents the order number of the Bragg peak. The image on the detector is blurred because of the spatial resolution of the detector and the slope error of the focusing mirror; here, the detector resolution is dominant if the focusing mirror developed by the author and collaborators is adopted [6,7]. Therefore, the wavelength resolution, $\Delta\lambda$, of the detector can be described as

$$\frac{\Delta\lambda}{\lambda} \sim \frac{\Delta x}{x},$$

where Δx is the spatial resolution of the detector. To simplify the calculation, the wavelength resolution arising from the width of the Bragg peaks is disregarded.

Figure 4 shows the wavelength and its resolution based on the detection position under the assumption that the parameters of the optics and detector in Figs. 2 and 3 are used, and neutrons with a wavelength of less than 0.4 nm are cut using the critical angle of the total reflection of a mirror, since the use of wavelengths below the Maxwellian peak of a neutron source is inefficient for neutron reflectometers. The primary peak includes the wavelength from 0.4 to 2.0 nm (solid red line) with a resolution of 2.5% to 0.5% (dashed black line), which are typical values for a neutron reflectometer. However, higher-order peaks emerged as the incident angle to the mirror increased, where the wavelength depends on the order of the Bragg peak and the detection position (solid lines), whereas the resolution is independent of the order (dashed line). A simple method to remove the contamination arising from the higher-order peaks is by using hardware, such as a mirror that filters short wavelengths based on the total reflection. Another approach is to subtract the higher-order peaks as follows:

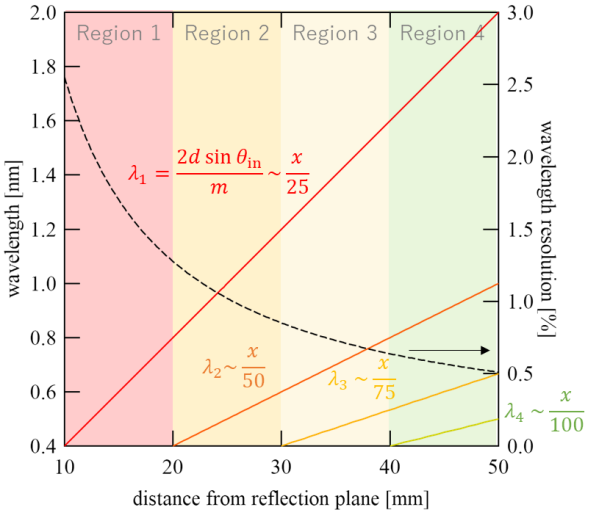

Fig. 4. Wavelength (solid lines, left axis) and resolution (dashed line, right axis) obtained by the novel polychromator for neutron reflectometry, in which the wavelength depends on the order of the Bragg peak, whereas the resolution is independent of the order.

As mentioned previously, only the primary peak was observed at a low incident angle to the polychromator (Region 1). As the incident angle increased, a second peak appeared in Region 2. The intensity of the second peak, $I(\lambda_2)$, can be evaluated using that of the primary peak in Region 1 if the normalizing factor is known. Similarly, the intensities of the third and fourth peaks in Regions 3 and 4, respectively, can be subtracted. Hence, the signal at x, $I(x)$, can be expressed as

$$I(x) = I(\lambda_1) + \sum_{m=2}^{4} a_m I(\lambda_m/m),$$

where a_m is the normalizing factor of the m-th peak, and the second term can be subtracted to evaluate $I(\lambda_1)$.

Finally, the intensity gain of the polychromator optics is evaluated and compared with that of the TOF method. The duty cycle of the TOF method is related to the wavelength resolution at the shortest wavelength as follows:

$$Duty\ cycle = \frac{\Delta t}{t_{max} - t_{min}} = \frac{\Delta\lambda}{\lambda_{max} - \lambda_{min}},$$

where t is the TOF; and the subscripts "max" and "min" represent the maximum and minimum wavelengths, respectively. Therefore, the duty cycle providing the same wavelength band and resolution as that of the polychromator is 0.625%. To compare the beam intensities, the product of the beam width, divergence, and duty cycle is evaluated. If the neutron density in phase space is uniform, then the product is proportional to the neutron intensity.

Table 1 lists the parameters for intensity comparison. To compare the flux at the same wavelength and resolution, a pixel of 0.5 mm for the shortest wavelength at x = 10 on the detector was extracted for the polychromator optics, which is the same as the spatial resolution. Because the distance between the mirror and detector is 1 m, the incident angle to the mirror is 10 mrad at x = 10. If the length of the mirror is 300 mm, then it functions as a slit of width 3 mm, and the divergence from the pixel to the mirror is 3 mrad. To

maintain the same optics as the polychromator optics, a slit of width 3 mm is placed instead of a mirror at the same position. The divergence from one slit to the other at the virtual source of the mirror is 40 mrad. The products of the parameters for each optics indicate that the polychromator optics possess a gain factor of 2, although this is only an estimation.

Table 1. Comparison of parameters related to intensity estimation. Products of parameters indicate that the polychromator optics possess a gain factor of 2.

	Duty cycle	Beam width	Divergence
Polychromator	100%	0.5 mm *on detector*	3 mrad. *to mirror with 300 mm length*
TOF	0.625%	3 mm *on a slit*	40 mrad. *to slit at virtual source*

3.2 Quasi-Elastic Neutron Scattering (QENS)

In the case of the reflectometer shown above, a polychromator is used to capture a spectrum of white beams under the assumption that no energy transfer occurs between the sample and neutrons. On the other hand, the dynamics of the sample can be obtained if the energy of the incident neutron is known. Here, an idea for a QENS instrument is presented as an example of neutron spectroscopy.

Figure 5 shows a schematic illustration of the QENS spectrometer utilizing the novel polychromator. The design is based on an inverse geometry spectrometer with a pulsed neutron source, such as the IRIS [10] and OSIRIS [11] at the ISIS, BASIS [12] at the SNS, and DNA [13] at the J-PARC MLF. Whereas a monochromator crystal is used as an analyzer in the conventional spectrometers described above, a novel polychromator is used in this study. For polychromating scattered neutrons in a sample, one focal point of the mirror is placed on the sample, and the other is placed on the PSD. In the conventional crystal, only the dynamics around the energy satisfying the Bragg condition of the crystal can be observed. Although the use of the polychromatic beam by a monochromator crystal are proposed [14,15], the energy band is very limited (less than ±10% from the center value). On the other hand, a wide energy band can be utilized in the polychromator, as will be discussed later.

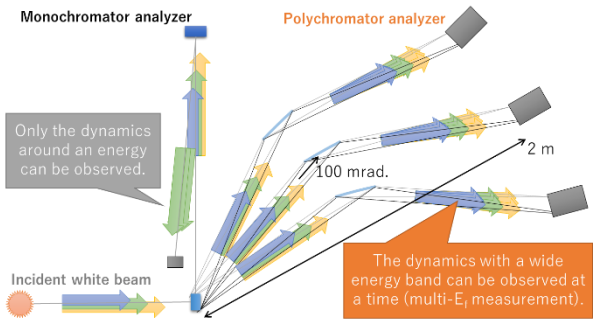

Fig. 5. Design of QENS spectrometer utilizing the novel polychromator based on an inverse-geometry spectrometer with a pulsed neutron source.

Figure 6 (a) shows the wavelength and resolution of the polychromator. The design of the polychromator differs from that of the neutron reflectometer, in that the angle of incidence that for reflectometry is 30 mrad at the center, whereas that of the QENS is 100 mrad. Combining the TOF enabled us to distinguish the higher-order reflections. Consequently, the wavelength from 0.4 to 2.0 nm was available without any gap by utilizing 10 Bragg peaks (shown as solid colored lines), in which the resolution was slightly higher than 0.3% at x = 80 and approximately 0.2% at x = 120 (shown as dashed line). Because the wavelength resolution arising from the pulse width was not considered, the value obtained was worse than those yielded by high-resolution instruments such as BASIS and DNA, i.e., 0.08% at λ = 0.63 nm based on Si(111) reflection. However, the important specification of the QENS spectrometer is not the wavelength resolution but the energy resolution, which limits the detection of slight changes in the width of a dynamic structure factor, which is described via a Lorentzian as a function of energy transfer for a relaxation mode. Because neutrons with longer wavelengths (i.e., lower energy) are available in the polychromator, a better energy resolution can be realized, even with the worse wavelength resolution.

To quantitatively evaluate the specifications of the QENS instrument, the relationship between the wavelength and energy of neutrons is used to estimate the energy resolution as follows:

$$E = \frac{h^2}{2m_n\lambda^2},$$
$$\frac{\Delta E}{E} = 2\frac{\Delta\lambda}{\lambda},$$

where m_n is the mass of a neutron, h is Planck's constant, and ΔE is the energy resolution. In addition, the energy window E_{window}, which limits the detection of significant changes in the width of a dynamic structure factor, are evaluated using as follows:

$$E_{window}(\lambda_m) = \frac{E(\lambda_{m+1}) - E(\lambda_m)}{2} - \frac{E(\lambda_{m-1}) - E(\lambda_m)}{2} = \frac{E(\lambda_{m+1}) - E(\lambda_{m-1})}{2}.$$

Figure 6 (b) shows the energy resolution (shown as solid colored lines) and window (shown as dashed colored lines) as a function of wavelength. The energy resolution is proportional to λ^{-2} or λ^{-3} when λ is scanned with m or x. The value of approximately 25 μeV at 0.4 nm decreased as λ increased to 1 μeV at 2.0 nm. The result shows that the energy resolution of 1 μeV is comparable or less than those yielded by BASIS and DNA. Notably, the resolution estimated in this study was based only on the detector resolution; in other words, the effects of the Bragg peak width of the multilayer and pulse width, which affect the TOF resolution, were not considered. However, the results demonstrated the potential of the polychromator for high-resolution QENS. Similar to the energy resolution, the energy window is proportional to λ or λ^{-2} when λ is scanned with m or x, and the value of approximately

1000 μeV at 0.4 nm decreased as λ increased to 200 μeV at 2.0 nm. The former value is comparable to that of the wide-window mode of DNA, and the latter value is comparable to that of the wide-window mode of BASIS.

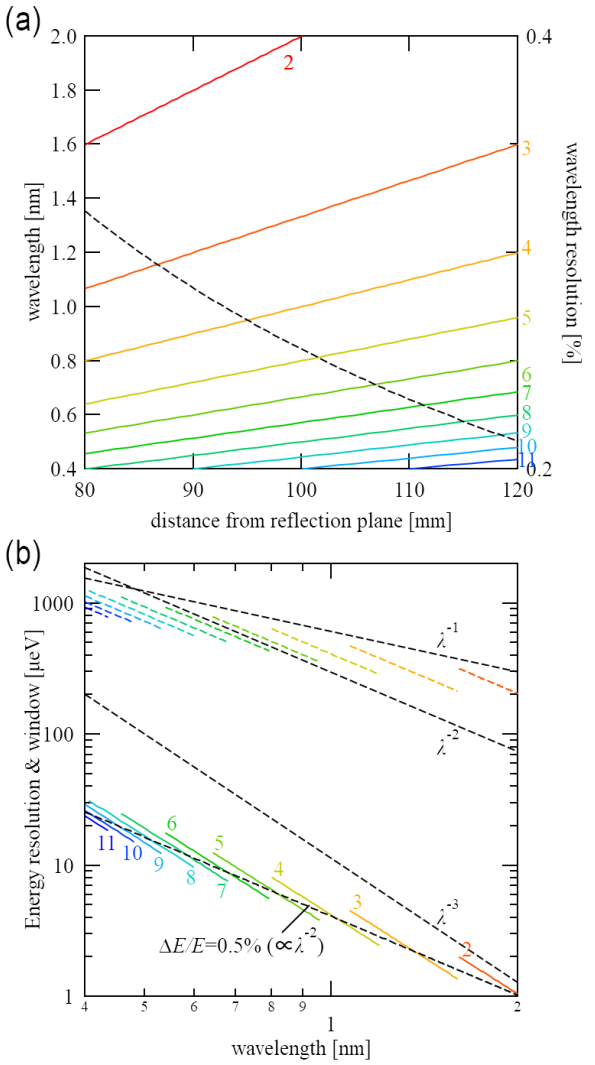

Fig. 6. (a) Wavelength (solid lines, left axis) and resolution (dashed line, right axis) yielded by the novel polychromator for QENS; (b) energy resolution (solid colored lines) and window (dashed colored lines) achieved by the polychromator design.

Therefore, we can conclude that the QENS spectrometer using the polychromator enables us to consider a wide energy range of white cold neutrons from 0.4 to 2 nm. Energy transfer with different energy resolutions can be measured simultaneously using different orders of reflection. This may facilitate peak width analysis for evaluating the width of energy transfer by considering the effect of resolution. Regarding the solid angle, a gap of 36 mm was required at the entrance of the analyzer mirror for a mirror length of 300 mm, where the maximum incident angle was 120 mrad. This resulted in a maximum coverage of the solid angle of 95% (36/38) under the assumption that analyzer mirrors with a thickness of 2 mm were placed around the sample, such as in the case of a radial collimator.

4 Conclusion

In this study, a novel polychromator comprising multiple layers on an elliptical mirror and a high-resolution PSD was proposed. One of the focal points of the mirror was placed on a virtual source, and the other was placed on the PSD. The spectrum of the white beam was observed on the detector as a function of the detection position owing to changes in the incident and reflection angles of the neutrons on the mirror. As the wavelength resolution of the polychromator is governed by the width of the Bragg peak, a "crystallic multilayer" with a large stacking number composed of materials providing less reflectivity in one layer unit was proposed to increase the crystallinity for sharp Bragg peaks. For the application of the polychromator, a neutron reflectometer with a continuous source and a QENS spectrometer with a pulsed source were designed, and their performances were estimated. The neutron reflectometer enabled us to measure the reflectivity over a wide momentum transfer range using a wide wavelength band, as in the TOF method. The QENS spectrometer encompassed an extremely wide energy range, i.e., from micro-electron-volts by extremely cold neutrons of λ = 2.0 nm, to meV by cold neutrons of λ = 0.4 nm. For the latter case, the proposed method demonstrated significant potential for improving the data quality via the application of higher-order reflections at the polychromator mirror. This is because the dynamic structure factor in an extremely wide energy transfer and momentum transfer space can be measured under different energy resolutions simultaneously. However, this is merely an estimation, and further research and development are required to demonstrate the actual performance of the polychromator in the future.

1. T. Matsushita *et al.*, Appl. Phys. Lett. **92**, 024103 (2008)
2. R. Cubitt *et al.*, J. Appl. Cryst. **51**, 257 (2018)
3. F. Ott and A. Menelle, Nucl. Instrum. Methods Phys. Res. Sect. A **586**, 23 (2008)
4. S. Takeda *et al.*, Opt. Express **24**, 12478 (2016)
5. T. Hosobata *et al.*, Opt. Express **25**, 20012 (2017)
6. T. Hosobata *et al.*, Opt. Express **27**, 26807 (2019)
7. F. Nemoto *et al.*, Nucl. Instrum. Methods Phys. Res. Sect. A **1040**, 166988 (2022)
8. A. Nelson, J. Appl. Cryst. **39**, 273 (2006)
9. L. G. Parratt, Phys. Rev. **95**, 359 (1954)
10. D. M. y Marero *et al.*, Physica B **150**, 276 (2000)
11. C. J. Carlile and M. A. Adams, Physica B **182**, 431 (1992)
12. E. Mamontov *et al.*, Neutron News, **19,** 22 (2008)
13. K. Shibata *et al.*, JPS Conference Proceedings **8**, 36022 (2015)
14. J. O. Birk, Rev. Sci. Instrum. **85**, 113908 (2014)
15. R. Bewley, Rev. Sci. Instrum. **90**, 075106 (2019)